Omkar Shende

ME 451B

Final Project

# Data Driven Analysis for Bypass-Transitional Boundary Layer

The transition to turbulence is a fundamentally complex topic, even when considering the standard modal analysis of exponential growth of Tollmien-Schlichting waves introduced into a flow at a set frequency. Bypass transition, which can lead to rapid laminar-to-turbulent transition, then, complicates matters even further and is a topic with a rich history, having been described as early as 1969 by Morkovin. It is often associated with the presence strong turbulent effects in the freestream of a wall-bounded flow, but Schmid and Henningson define bypass transition as fundamentally distinct from standard transition, as it is predicated on "[emanations] from nonmodal growth mechanisms." [1] That is, it is not a single mode of disturbance that causes the initial instability, and critically, because it depends on free-stream interactions with the wall, analysis cannot just be confined to the wall region.

Given such a broad definition, pinning down the mechanisms that cause and control bypass transition is an area of active research. Active research in recent days in fluid dynamics has also been directed into machine learning methods for fluid flows using unsupervised methods like neural networks, but an interesting counterpoint to this vein of research are data-driven methods that seek to extract coherent structures from the flow for the creation of models. In particular, the spectral proper orthogonal decomposition (SPOD) and dynamic mode decomposition (DMD) are two methods of examining flows that vary in space and time in a domain and can lead to lower-rank approximations of the dominant modes of the said flow. In particular, Alessandri, *et al*. [2] use DMD as a method of classifying the nominally laminar, transitional, and turbulent regions of a flat-plate boundary layer with a strong adverse pressure gradient using particle image velocimetry data of the wall-normal and streamwise velocity components. This work will examine a higher Reynolds number transitional boundary layer explicitly undergoing bypass transition and apply the methods in Alessandri, *et al*. and examine their results in fully three-dimensional flow. Then, having followed the definitions in [2], the SPOD and DMD modes in each of the three regions will be examined and the differences between each will be highlighted.

For this work, streamwise and wall-normal velocity data will come from the transitional boundary layer provenance at the Johns Hopkins University turbulence database collected at [3], which contains state

information for an incompressible statistically stationary direct numerical simulation of flow over a flat plate with a Reynolds number (with respect to the plate length) of 840,000 and a freestream turbulence intensity (FSTI) of 3%. These parameters match the canonical T3A transition experiment and are somewhat comparable to the conditions of $40{,}000 < Re < 90{,}000$ and $0.65\% < FSTI < 2.87\%$ measured experimentally in [2], but this setup does not have the strong flow separation due to an adverse pressure gradient observed in the experimental paper, and so we will not compare the analysis results from this work to those from [2]. Figure 1 shows a schematic of the computational domain and coordinate system, with the data region enclosed by the red box.

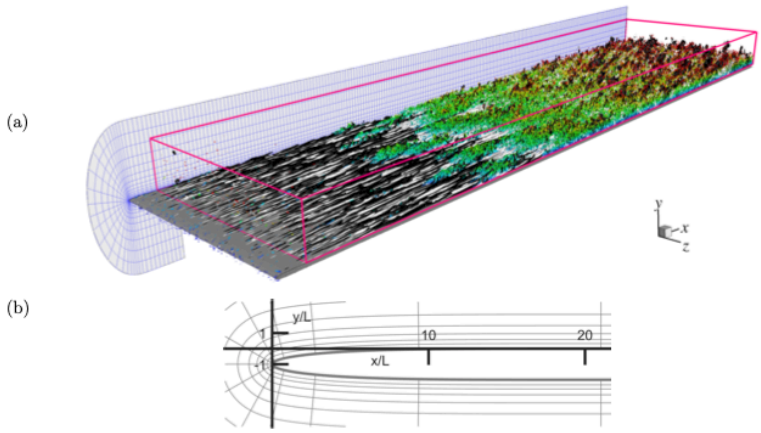


Figure 1: (a) Visualization of the computational domain for the boundary-layer simulation. (Color) Vortical structures, $\lambda_2 = -0.01U_\infty^2/L^2$; streamwise velocity fluctuations, (black) $u' = -0.1U_\infty$ and (white) $u' = 0.1U_\infty$; (side view) computational grid (every sixteenth grid line is plotted). The rectangular box marks the domain stored in the JHTDB. (b) Origin of the coordinate system.

*Figure 1: Domain image and coordinate system from [3]*

SPOD is a well-established technique, having been first proposed in the last century to find optimal spatiotemporal coherent structures for stationary flows. Spatial proper orthogonal decomposition finds the optimal spatial modes for a single snapshot in time and is accomplished by taking the singular value decomposition of each snapshot and finding each rank-one mode. SPOD incorporates time correlation as well and the specific SPOD algorithm being used in this work comes from published code from [4], which uses Welch's method as part of the algorithmic structure to find spatiotemporal coherent structures in flows. In particular, the data is first partitioned into $M$ blocks of $k$ temporal snapshots. The data from each of these $M$ blocks are stacked into a column vector $X_{m,i}$ and combined to a full state matrix $\boldsymbol{X_m}$. This matrix is discretely Fourier transformed in time and based on the number of blocks of snapshots in time, $M$ Fourier-transformed $\widehat{\boldsymbol{X}}_{\boldsymbol{m}}$ matrices are formed.

$$\boldsymbol{X_m} = \begin{bmatrix} | & | & | & | \\ X_{m,1} & X_{m,2} \dots X_{m,k-1} & X_{m,k} \\ | & | & | & | \end{bmatrix} \xrightarrow{DFT} \widehat{\boldsymbol{X}}_{\boldsymbol{m}} = \begin{bmatrix} | & | & | & | \\ \widehat{X}_{m,1} & \widehat{X}_{m,2} \dots \widehat{X}_{m,k-1} & \widehat{X}_{m,k} \\ | & | & | & | \end{bmatrix}$$

Then, for every computed frequency, POD is carried out to find the optimal ranking of the $M$ modes, using an inner product defined by the user; as a result, for each frequency the modes are orthogonal to each other. For this problem, since the data are velocity components and each grid point occupies the same volume in space, a simple identity norm will be sufficient, but *a priori* knowledge of grid weights or enthalpy considerations for forming an energy norm, for example, can come into play here. Most of parameter values used are the defaults from the code in [4], which may not be optimal.

Like SPOD, DMD is a completely general method, and [5] goes into its many applications beyond fluid dynamics. For DMD, let us consider $k+1$ temporal snapshots of the flow that have been made into column vectors, each denoted $X_i$, which can consist of more than one velocity component or other variable. We can then form two matrices collecting all this state data as

$$\boldsymbol{X} = \begin{bmatrix} | & | & | & | \\ X_1 & X_2 \dots X_{k-1} & X_k \\ | & | & | & | \end{bmatrix} \quad \boldsymbol{X'} = \begin{bmatrix} | & | & | & | \\ X_2 & X_3 \dots X_k & X_{k+1} \\ | & | & | & | \end{bmatrix},$$

where each state vector $X_i$ is tall and skinny. DMD tries to find the best possible linear operator, $\boldsymbol{A}$, mapping these two Hilbert spaces such that $\boldsymbol{X'} \approx \boldsymbol{AX}$. However, since in principle this means the operator could be massive for discrete datasets, all that is computed will be some subset of the eigenvalues and eigenvectors of $\boldsymbol{A}$, and there are a few different variations on how to find these quantities. The eigenvectors form the DMD modes, while the eigenvalues give the frequency and growth rate of those modes in space. Using this reduced ranked approximation, we can also construct a reduced rank approximation of the operator and find the $L_2$ error associated with the estimated future state and $\boldsymbol{X'}$.

The primary different use of DMD versus SPOD is that DMD allows for the reconstruction of the state at any future time, which is useful from a controls perspective, as it creates a linear model of a potentially chaotic nonlinear system. Both DMD and SPOD are agnostic to the governing equations and grid structure, and so can be applied without any *a priori* knowledge about the flow. SPOD, however, only gives general information about the spatiotemporal evolution of structures, without specific dynamics. The specific DMD algorithm being used in this report comes from published code from [5].

To perform the analysis, a $(N_x, N_y, N_z) = (500, 28, 28)$ rectangular subset of the total domain from [2] will be examined across 320 snapshots, with dimensions chosen to stay within the memory limits of the MATLAB program being used for this analysis when using single precision floating point numbers. Care was taken to pick a spatial and temporal span where isolated turbulent spots were not active, as it does not appear [2] sought to study this phenomenon, and to include data from the freestream region.

To classify regions of the flow, the procedure used by [2] iteratively examines the DMD modes of the flow by increasing the streamwise extent of the data fed into the analysis side, starting from the first point to the full number of points in the streamwise direction. The residual between the true measured flow state and the DMD-based prediction, $||\boldsymbol{X'} - \boldsymbol{AX}||$, can be calculated. Across the streamwise grid points, we consider the point with the lowest error value to be the start of the transitional zone, as it is where the nominally laminar inflow condition begins breaking down, and the DMD operator built in a linear context fails to predict the instability growth. From this point, denoted $k_1$, the error increases monotonically, with a kink occurring between two linear regions of growth at a point $k_2$. Fitting one line from $k_1$ to $k_2$ and one from $k_2$ to $N_x$ will yield some error measures. Finding the $k_2$ value that minimizes the sum of the fitting error of the two lines will be the optimal division between the transitional and turbulent regime.

The variable of interest for [2] to identify zones is the wall-normal velocity, which is most important when considering Orr-Sommerfeld stability analysis; indeed, since [2] uses experimental data from a single spanwise plane, it can be argued [2] explicitly invokes Squire's theorem to conduct purely two-dimensional mode analysis. The key feature of [2] is that it modifies the DMD procedure such that columns of the state matrix are not individual temporal snapshots, but snapshots ordered by streamwise position. In this way, we can find the *spatial* growth rates, modes, and frequencies, as opposed to the temporal ones. For completeness, the standard temporal DMD is also performed in this report.

In addition, since the streamwise fluctuating velocity contains most of the energetics, the DMD analysis for identifying zones will be considered with both streamwise and wall-normal velocities. In figure 2(a) and 2(b), the results of the analysis using five computed modes are shown with the dashed vertical lines approximately marking the three demarcated zones, and in figure 2(c), the actual illustration of the linear fitting process from [2] is shown. The actual grid points identified between the two scenarios are almost the same, but since it incorporates more information, the transition points given by figure 2(a) using two components and the apparently more robust temporal DMD formulation (in blue) are used.

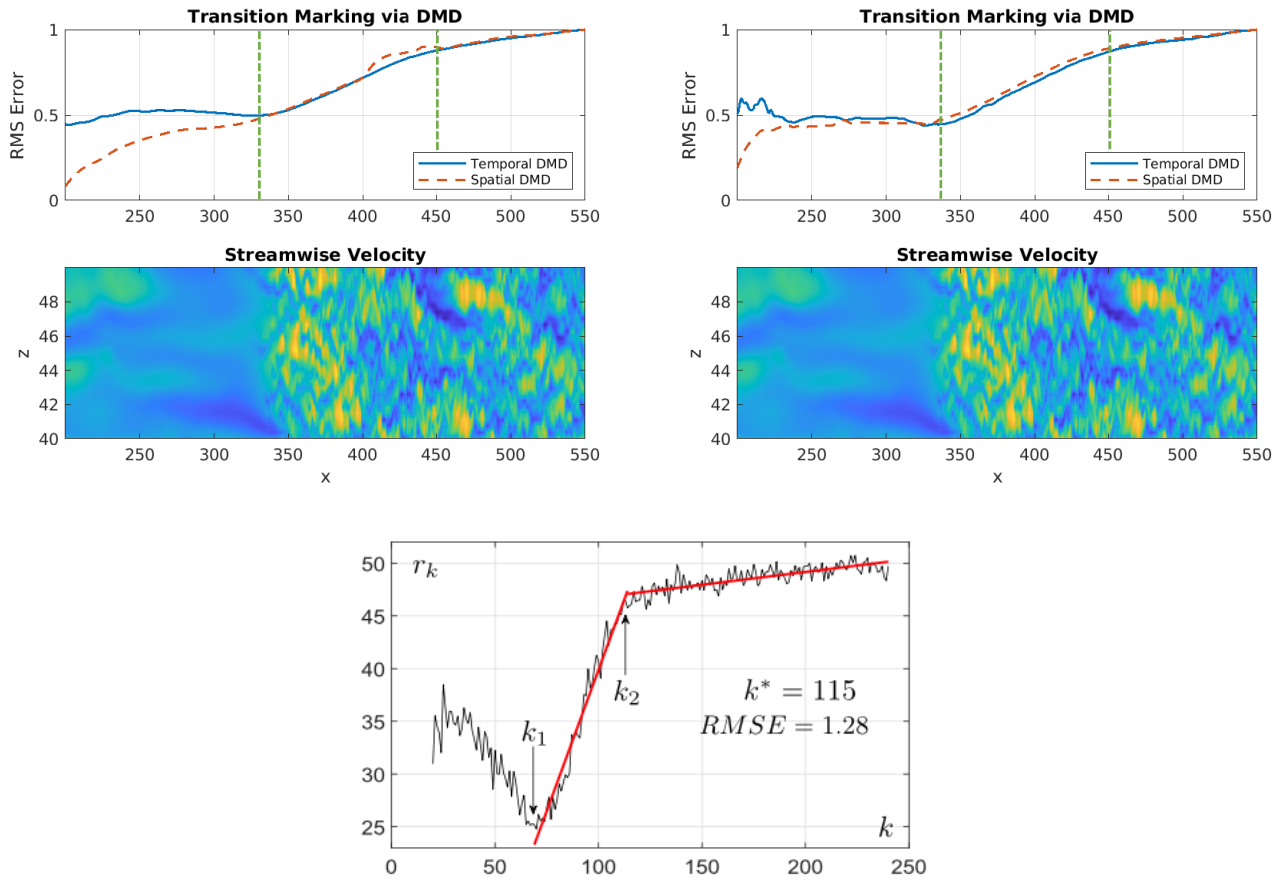


*Figure 2: Clockwise from top left; (a) Results of the DMD procedure on the dataset using both u' and v' with spatial and temporal DMD results, and an instantaneous snapshot of the streamwise velocity fluctuations; (b) Results of the DMD procedure on the dataset using just v' with spatial and temporal DMD results, and an instantaneous snapshot of the streamwise velocity fluctuations; (c) The results of the DMD procedure as shown in [2], which highlights how the linear fit is conducted.*

Having found the three separate regions of interest, we can find the Ritz and continuous eigenvalues corresponding to the most unstable modes for the two-component velocity fields to find the most dominant temporal and spatial instability growth rates in each region. While we will discuss the regions in detail, this information is summarized in in Table 1. Each DMD problem uses the top 95% of available modes to reduce spurious values, but some convergence issues were still encountered. In region 1, the flow is temporally unstable, and at best neutrally stable in the spatial sense. In regions 2 and 3, the flow is at best neutrally stable in temporal evolution and possibly stable in spatial evolution. As bypass transition seems to be driven by convective instabilities, having the instability growth be larger upstream seems intuitive.

| $Re(\omega)$ | Region 1 | Region 2 | Region 3 |
|---|---|---|---|
| Temporal | 0.2113 | 0.0333 | 0.0716 |
| Spatial | 0.0114 | -0.0088 | -0.0120 |

*Table 1: The maximum growth rate for each region and analysis types given by the DMD modes*

In region 1, which corresponds to the area where the boundary layer is nominally laminar, we expect the influence of the free stream to be the cause of instability, and we indeed see that in figure 3(a), the strongest $y$-velocity structures averaged across the spanwise direction from the first 40 modes are far above the wall. In 3(b), we can also see that the modal energies for SPOD are well separated, and the Ritz eigenvalues are not uniformly close to the unit circle. Energy is concentrated at low frequencies, which is what we'd expect for a receptivity problem driven by energy from the freestream.

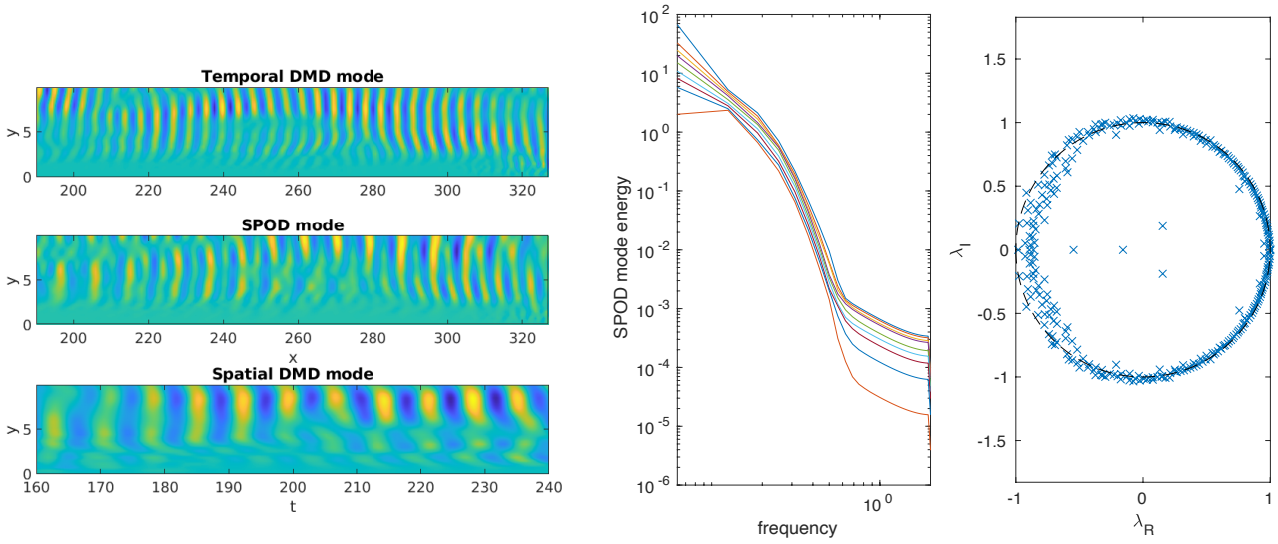


*Figure 3: For region 1; (a) at right, the first temporal DMD mode and SPOD mode at a corresponding frequency, and the first spatial DMD mode; (b) at left, SPOD modal energies and DMD Ritz eigenvalues*

In the second region, we expect the flow to be transitioning to turbulence via interaction with the free-stream, and we see that the eigenvalues in figure 4(b) are much more evenly distributed in phase, and possibly due to energy transfer, the modes at low frequencies are much more comparable in magnitude. In figure 4(a), we also see that the wall-normal velocity structures averaged across the span are stretching much closer to the wall, and while the frequency of the temporal modes (*i.e.*, the spacing of the mode

peaks) appears similar that in figure 3(a), the energetics are more concentrated closer to the wall as perhaps part of a lift-up or vortex-shedding mechanism.

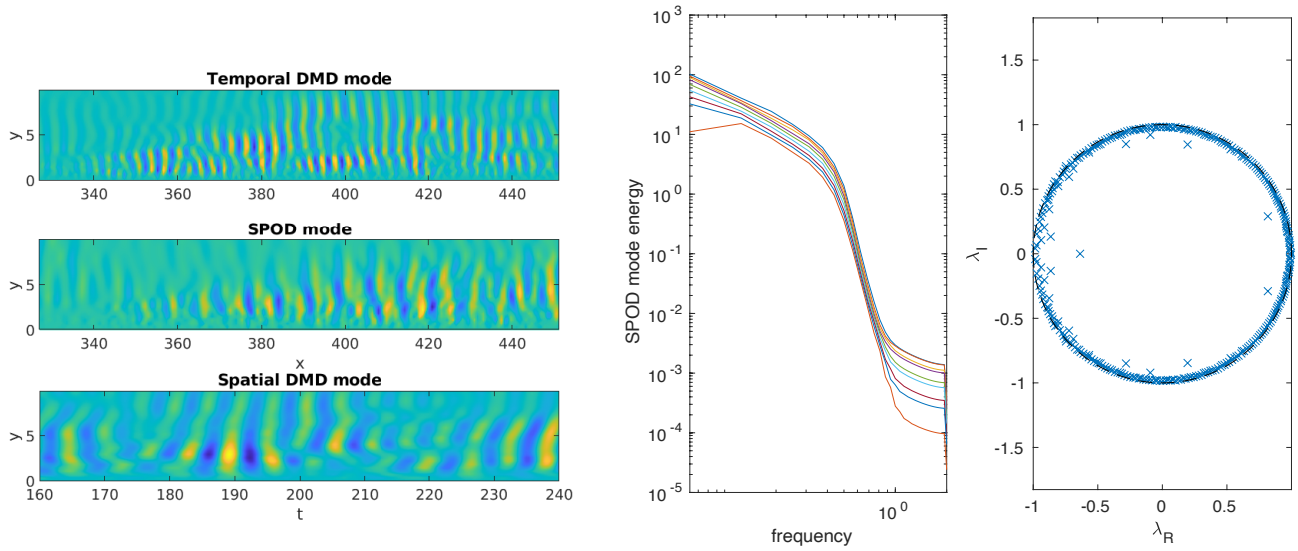


*Figure 4: For region 2; (a) at right, the first temporal DMD mode and SPOD mode at corresponding frequency, and the first spatial DMD mode; (b) at left, SPOD modal energies and DMD Ritz eigenvalues*

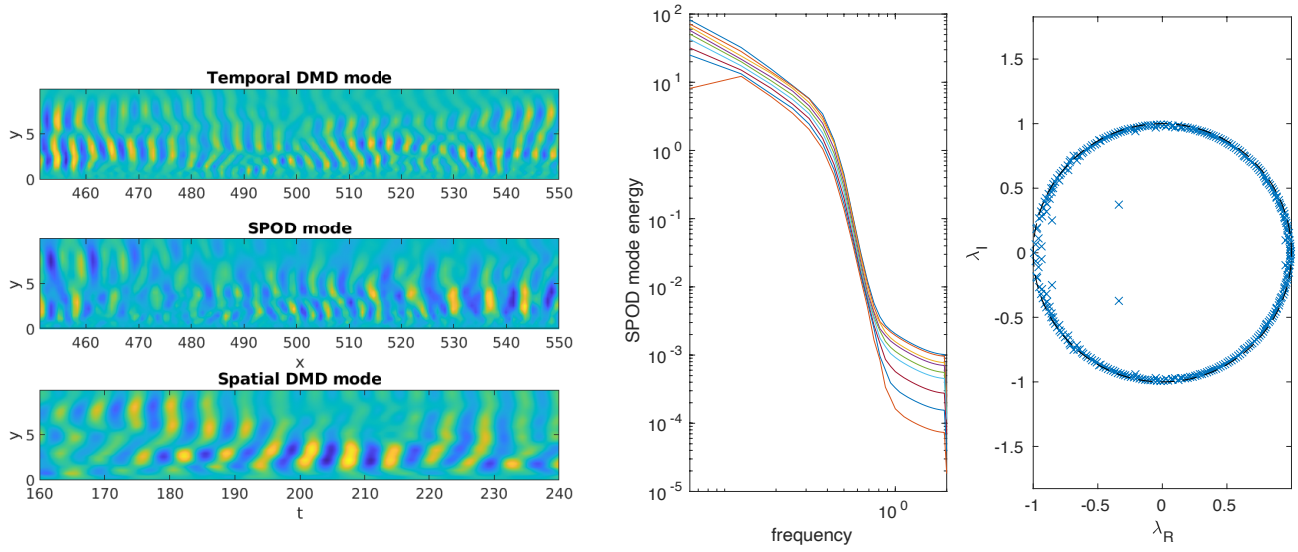


*Figure 5: For region 3; (a) at right, the first temporal DMD mode and SPOD mode at a corresponding frequency, and the first spatial DMD mode; (b) at left, SPOD modal energies and DMD Ritz eigenvalues*

In the third fully turbulent section, we see the eigenvalues in figure 5(b) are more clearly aligned onto the unit circle, indicating a broadband spectrum probably exists now. Furthermore, we see that in figure 5(a) that spanwise-averaged vertical velocity structures span the entire wall-normal distance and show higher frequency content than can be seen in figure 2. There is also more intermittency, which is classically a symptom of turbulent activity. As a closing note, the DMD and SPOD modes are fundamentally three-dimensional and for both velocity components, even though a spanwise-averaged overview of the wall-normal velocity field is the focus of figures 3-5.

We see that the three regimes are dynamically different and can track the growth of structures toward the wall. Using both temporal and spatial DMD analysis has let us find linear growth rates (and, while not shown here, phase speeds as well), and since we are under-resolving the velocity field by not using the full DNS resolution, we are likely capturing the large-scale dynamics of the flow and removing the nonlinear effect of the small-scale fluctuations. [2] further makes the case that the DMD classification used herein matches well with classical transition markers. A tangent that is not explored in this report, but is easily accessible with existing tools, is examining whether the eigenvalues of just the streamwise or just the wall-normal velocity follow the same trend as for the combined system of two components.

As a final aside, as might be suggested by figures 2-4, SPOD and DMD analysis have many similarities with each other, a point explicated fully in Towne *et al*. [4] In particular, that work shows that SPOD modes are optimal DMD modes, if the DMD process is run on an ensemble of different realizations of a stationary flow process. That is, each DMD mode has associated with it a frequency; if SPOD were run on the flow and the frequencies were matched between the two decompositions, a particular DMD mode would be some linear combination of the SPOD modes at that frequency. DMD might be considered nonmodal analysis of SPOD modes, as a result. While DMD has the benefit of providing a linear operator that can be used to forecast the future state of the system, SPOD is more robust and provides more insight into the most important modes of the system, if considering modelling. This is because for each frequency, the modes are ordered; DMD does not give any such guaranteed ordering.

Another flow decomposition method that has recently become tractable is resolvent analysis, which finds an optimal linear operator that maps the output response of a flow's fluctuating velocity fields based on the instantaneous nonlinear interactions of those fluctuations. Once this operator is found, a singular value decomposition can be applied to find independent input and output modes from the two sets of singular

vectors. While the input modes, that is, the modes that indicate which types of disturbances are most amplified, must be calculated, Towne *et al*. [4] show that if one considers the Navier-Stokes equation to be forced with uniform white noise as a disturbance, the resolvent modes will be the same as the SPOD modes. While it will not be discussed in detail, a possible way to examine the disturbances further is shown in [6], which allows one to find the eigenbases of the disturbances and the mean base flow directly. The SPOD modes, however, can be calculated without knowing the flow base state or governing equations, since the mean base state would appear as a zero-frequency mode.

In conclusion, an interesting method for algorithmically defining transition on a flat-plate boundary layer has been explored, and the use of DMD and SPOD algorithms to analyze the flow in the full spectrum of the laminar-to-turbulent regime via bypass transition has been shown. In places where the flow is highly turbulent, some basic principles from linear stability analysis can still be applied, and since [2] did not consider the three-dimensionality of the velocity fields or mode shapes for the streamwise velocity field, those visuals were not included herein, but could also be studied. Future directions for this work could include mapping scalar quantities like the Q-criterion or spanwise-oriented vorticity to better mesh with existing transition literature. Such scalar analysis can be implemented using DMD or SPOD without knowledge of the governing equations. Using higher frequency and higher resolution spatial data would also better capture all relevant structures, but the use of DMD and SPOD with even sparser data shows promise in analyzing large-scale energetics of turbulent flows.

[1] Schmid, P. J., *et al*., *Stability and transition in shear flows*. Springer, **2001**.

[2] Alessandri, A., *et al*., *Dynamic mode decomposition for the inspection of three-regime separated transitional boundary layers using a least squares method*. Physics of Fluids 31, 044103, **2019**.

[3] turbulence.pha.jhu.edu/docs/README-transition_bl.pdf

[4] Towne, A., *et al*., *Spectral proper orthogonal decomposition and its relationship to dynamic mode decomposition and resolvent analysis*, J. of Fluid Mech. 847, 821–867, **2018**.

[5] Kutz, J. N., *et al*., *Dynamic Mode Decomposition: Data-Driven Modeling of Complex Systems*. Society for Industrial and Applied Mathematics, **2017**.

[6] fluids.ac.uk/files/meetings/Resolvent-applications_McKeon.1575555382.pdf